Edge channels and the quantum-Hall-effect breakdown

A. A. Shashkin,* A. J. Kent, P. A. Harrison, L. Eaves, and M. Henini
Department of Physics, University of Nottingham, University Park, Nottingham NG7 2RD, United Kingdom
(Received 1 June 1993; revised manuscript received 8 November 1993)

Quantum Hall devices have been investigated in the regime of the breakdown of dissipationless current flow by means of a photoresistance imaging technique. It is possible to distinguish three stages in development of the breakdown: (i) the initial rise of the longitudinal resistance due to a change with the Hall electric field of the percolation threshold leading to electron backscattering between the edges; (ii) at higher bias currents a strong response from the edges is observed in two-dimensional images, in agreement with the edge-state model; (iii) on increasing the bias current further, electron heating effects are seen to prevail.

I. INTRODUCTION

The integer quantum Hall effect (QHE) in a two-dimensional (2D) electron gas in high magnetic fields has been the subject of considerable interest for more than a decade. The transport properties of a conventional long Hall bar are characterized by the disappearance of longitudinal resistance and corresponding quantization of the transverse (Hall) resistance at filling factors close to integer values.[1] The high precision of Hall voltage quantization means that such devices can form the basis of international resistance standards. Improved precision of the measurement can be achieved by passing higher currents through the device. However, as the current is increased a point is reached where the longitudinal resistance breaks away from zero and the Hall resistance is no longer accurately defined in terms of the fundamental constants. This effect is known as the breakdown of the quantum Hall state.

QHE breakdown in macroscopic samples has been intensively studied (e.g., [Refs. 2–12) but up to now its mechanism has not been identified unambiguously. A number of mechanisms for the breakdown have been proposed over the years. These include the following: (a) Thermal instability, whereby the rate of gain of energy by the electrons exceeds their ability to relax by transferring energy to lattice modes.[2,3] Heating of the electrons eventually lead to inter-Landau-level transitions; (b) Spontaneous emission of phonons when the electron drift velocity exceeds the velocity of sound in the substrate material;[4,5] (c) Injection of nonequilibrium electrons from the current contact;[6] (d) Quasielastic inter-Landau-level scattering accompanied by acoustic-phonon emission at large values of Hall field;[7–9] (e) Change of the mobility threshold in the Hall electric field;[10] (f) Interedge state tunneling and backscattering;[11] (g) Successive breakdown of small localized inhomogeneous regions within the device[12] due to any of the above processes. All of these processes have their own particular spatial dependence: Mechanism (a) would be expected to start near the current entry and exit points and spread through the bulk while (b), (d), and (e) are bulk effects. Mechanism (f) would take place at the sample edges and show dependence on magnetic field and current polarity and (g) could start anywhere within the sample depending on the particular sample chosen. Theoretically estimated values of the critical current for the breakdown are appreciably higher than those observed in experiment. This fact is usually attributed to sample inhomogeneity.

It is clear that a spatially sensitive probe would be able to discriminate between these mechanisms. The positioning of the potential probes at various places around the edge and within the device is one way to achieve spatial resolution of the transport properties. However, one must be very careful doing this because any process that relies on a nonequilibrium population of edge channels, for instance, will be affected by the probes which act as reservoirs to equilibrate the distribution. In addition, disturbance of the original potential fluctuations occurs.

The technique we describe in this paper uses a movable optical probe to stimulate breakdown to a localized region of a conventional Hall device. The technique is nondestructive and no special processing of the device is needed, which means that it can be used to characterize a sample prior to its use as a conventional Hall standard, for example.

The aim of the present work is to investigate the breakdown mechanism of QHE and to find out the role of edge currents in the breakdown regime.

II. EXPERIMENTAL TECHNIQUE

The experimental arrangement is shown in Fig. 1. The sample is located in an optical access cryomagnetic system at a temperature of 1.5 K and a magnetic field of up to 7 T. The beam from a 0.5-mW He-Ne laser ($\lambda=633$ nm) is chopped at a frequency of about 1 kHz using an acousto-optic modulator and is focused to a spot about 20 μm across on the top surface of the sample. A pair of computer-controlled galvanometer mirrors allows positioning of the laser spot anywhere on the device. With a constant bias current I applied to the device source-drain contacts, a component of the longitudinal voltage in phase with the beam modulation is picked up by the potential probes. This signal is fed to the input of a lock-in amplifier and then recorded by the computer as a function of the mirror positions, thereby creating a 2D image of the strength of the photoresistance effect.[13]

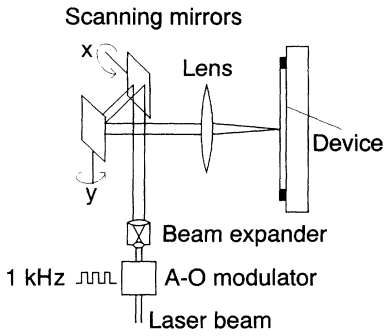

FIG. 1. The laser beam is chopped by an acousto-optic modulator and positioned on the top of the sample using a pair of galvanometer driven x-y mirrors under computer control. A bias current is passed through the sample and the component of the longitudinal voltage in phase with the beam modulation is measured.

The sample is based on a GaAs/AlAs heterojunction and is rather special in that the doping and the width of the doped layer are small. As a result, the sample is free from a parallel conducting channel, even under daylight illumination. This is essential in an experiment where we intend to observe the effect of illumination on the 2D-layer resistance. Figure 2(a) shows the layer details and the corresponding band diagram. Standard rectangular Hall devices were defined by etching. They had active areas 1.2 mm$\times$100 μm and 2.4 mm$\times$280 μm, see Fig. 2(b). The values of 2D electron density were about 4.2×10^{15} m^{-2} under illumination and the mobility $\sim$100 m^2 V^{-1} s^{-1}. Figure 3 shows the longitudinal resistance as a function of magnetic field with the sample in daylight. The absence of any parallel conduction is clearly evident and the illumination gives rise to only a slight increase in 2D electron-gas areal density. This increase in density is saturated within a short period of illumination and is persistent after switching off the illumination. In the remainder of the paper, we consider the dynamic effect of laser illumination on the electrical resistance of the sample.

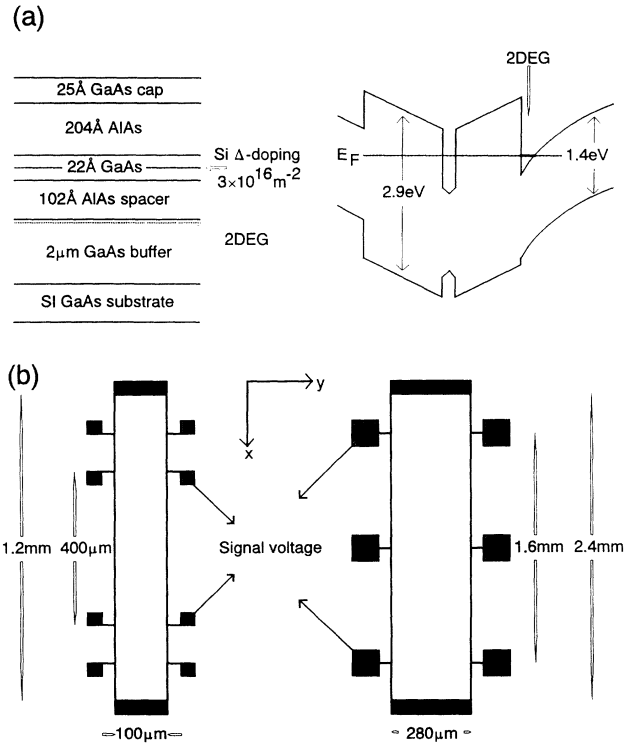

FIG. 2. (a) Cross section of the heterojunction and the band diagram. 2D electrons are supplied by the Si δ layer. The AlAs band gap shown in the Γ-valley conduction-band confining potential. (b) Geometry of samples used in measurements. Experimental results displayed in the following figures were obtained using the potential probes indicated. Axes indicate the scanning directions.

Radiation from the He-Ne laser (photon energy $h\nu=1.96$ eV), incident on the top of the device, penetrates the AlAs ($h\nu$ is less than the X and Γ valley bandgaps) and is absorbed by the GaAs (band gap $=1.6$ eV) creating electron-hole pairs to a depth of about 1 μm. A proportion of the electrons find their way into the 2D layer increasing the local areal density slightly. Knowing the laser power incident on the sample, $P_{\rm opt}\approx2$ μW, and the electron-hole recombination time τ it is possible to estimate the local increase in electron density ΔN_s. Time-resolved photoluminescence measurements[14] give the electron-hole recombination time in the bulk of GaAs $\tau\sim1$ ns, which yields $\Delta N_s\sim2\times10^{11}$m^{-2} and represents an increase of the order of 1%.

A secondary effect of absorption of the laser light is a slight warming of the region being probed. Equating the

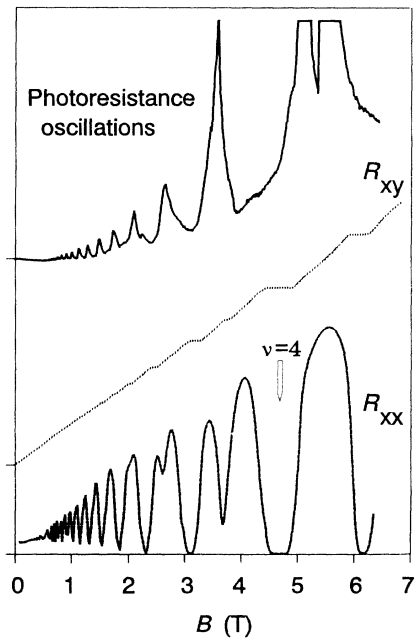

FIG. 3. Magnetic-field dependence of the resistances R_{xx} and R_{xy} on the wide sample at bias current of 1 μA. The sample was in daylight. An example of photoresistance oscillations $\delta R_{xx}(B)$ at bias current of 100 μA when the light spot is near the sample edge is also shown.

rate of energy input to the region probed with the rate of energy loss by thermal conduction of the surrounding areas, we estimate the increase in temperature to be ~ 10 mK at $T=1.5$ K, which is negligible. Hence, in the absence of parallel conduction and any significant heating effects, the effect of the optical excitation is to cause a small ($\sim 1\%$) increase in the areal density of the 2D electron gas and a corresponding increase in the local Fermi level.

Macroscopic inhomogeneity of the samples is always a big problem in transport measurements. This can be roughly estimated by using different pairs of potential probes. To check the homogeneity of the samples, we employed our space-resolved technique which is far more sensitive in determining the quality of the sample.

III. RESULTS

In the experiment described here we worked at an integer filling factor $\nu=4$ where the resistance R_{xx} measured in the linear regime displays a rather wide minimum (Fig. 3). The variation of the resistance R_{xx} with source-drain current I is shown in Fig. 4 for two samples having different widths. The dependence of the resistance on current I is qualitatively similar for all samples used. One can distinguish three characteristic ranges of current on the experimental curves: (i) a quite sudden onset of breakdown indicated by the longitudinal resistance departing from zero; (ii) the rate of increase of R_{xx} with current slows; (iii) at much higher currents the increase speeds up again. The arrows in Fig. 4 roughly mark the boundaries between these ranges. We will see below that the experimental images are also qualitatively different in the three regions in question.

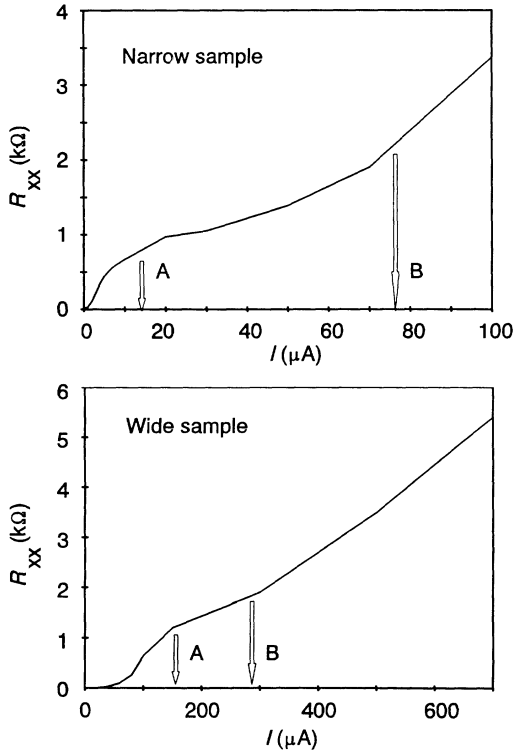

FIG. 4. Breakdown curves for the narrow and wide samples. The values of $R_{xx}(I)$ are averaged at two current directions. These were slightly dependent on magnetic-field and current polarity, however the reversal of magnetic-field or current direction did not influence the characteristic shape of the breakdown curve. Arrows A and B roughly indicate boundary currents at which the behavior of the breakdown curve changes.

A sequence of images taken on the narrow and wide samples are shown in Figs. 5 and 6, respectively. A light area in the image indicates an *increase* of the longitudinal resistance as a result of illumination. In the low-current region one can see the strong response from an area within the bulk of the device; the extent of this area increases as the current is raised. At currents corresponding to a region on the breakdown curve $R_{xx}(I)$ around the maximum slope, the active area occupies the whole sample. Reversal of current or magnetic-field direction was found to have a weak effect on the responsive area. This weak effect is less noticeable in the case of the wider, less homogeneous sample (Fig. 6).

As the current is increased beyond the knee in the breakdown curve, the curve of the images changes. We see that the two edges respond: illumination at one edge gives rise to an increase in resistance while that at the other edge triggers a decrease in resistance. Interestingly, the polarity of the responses reverses with changing either the magnetic-field or current directions, as shown for the wider sample in Fig. 7, but illumination at the edge with higher electron potential *always* results in increasing resistance R_{xx}. The resistance *decreases* when the edge with lower electron potential is illuminated. The distance across a sample between lines corresponding to maximum (positive and negative) changes in the longitudinal resistance is less than the sample width due to a finite-length scale of the confining potential at the edges, as was considered in Ref. 13. These effects are more pronounced in the case of the narrow, more homogeneous, sample.

In this region of the breakdown curve, and also in the low-current region, the sample responds when the light spot is between the potential probes used. The form of the images is independent of which pair of potential probes was chosen to measure R_{xx}.

Further increase of the bias current leads to the disappearance of the edge effect in the narrow sample. An area corresponding to the decrease in the longitudinal resistance spreads out across the sample and becomes dominant (Fig. 5). The influence of magnetic-field and current directions on the images diminishes as well. The light regions of the image near the source and drain contacts are presumably a contact effect. It was not possible to achieve a sufficiently high current to observe the disappearance of the edge effect in the wide sample.

It is clear that the behavior of the images is considerably different in the different regions of the breakdown curve. In the low-current and high-current regions we see a response from the bulk of the sample that is not drastically influenced by the change of current or magnetic-field polarity. In the intermediate region of bias currents the dominant response comes from the edges.

The polarity of variation in the longitudinal resistance is opposite when illuminating the opposite edges and changes upon reversal of either magnetic-field or current direction.

When the magnetic field is swept with the light spot at a fixed point on the sample surface we observe photoresistance oscillations similar to Shubnikov–de-Haas oscillations. An example of the photoresistance oscillations is shown in Fig. 3. Since such oscillations probe a local electron density in the sample, these enable us to estimate a change in the electron density caused by the bias current.[15] For example, for the wide sample the change of N_s at the edge was about 8% at a current $I=400$ μA and a filling factor $\nu=4$.

We note that the two boundary currents between the three ranges (see arrows in Fig. 4) roughly correspond to those at which at first Shubnikov–de-Haas (arrow A) and then photoresistance (arrow B) oscillations vanish with raising the bias current through a sample.

IV. DISCUSSION

We will start by considering the range of currents in which the edge effect is observed. As was shown in Ref. 13 the scale of potential-well bending at the edge is about 20 μm in our samples. Therefore, one can assume[16] that Landau levels behave at the edge as shown in Fig. 8. The measured longitudinal resistance should be sensitive to inter-Landau-level transitions that occur more easily at the edges due to the bending of Landau levels. Hence, one can expect the edge effects to be seen in the images.

We can interpret the origin of the edge effect at integer filling factors as follows: As long as the QHE breakdown has already started, there is the backscattering of electrons between the opposite edge channels. At sufficiently low bias currents the corresponding transverse current between edges (henceforth called the backscattering current) flows at the Fermi level, as will be discussed below. In accordance with the current continuity condi-

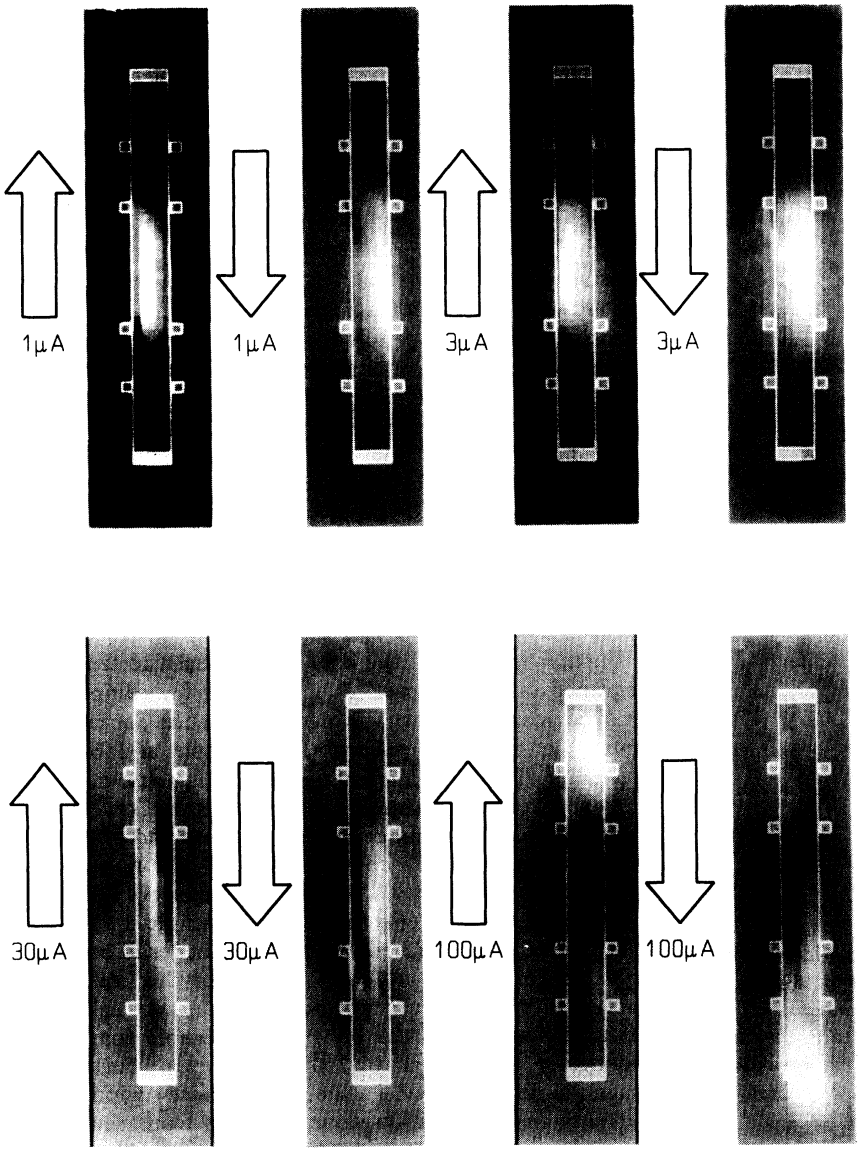

FIG. 5. A set of experimental images taken on the narrow (100-μm wide) sample at the indicated bias-current direction and size. The magnetic field of 4.6 T is directed into the plane of the diagram. White and black regions correspond, respectively, to an increase and decrease in R_{xx}; the zero level can be judged by looking at the shade at a position well outside the etched region. The images were taken at a resolution of 20 μm (five points across the width of the etched area). Sample contours with potential probes are also shown. It is noticeable that the presence of potential probes, even unused ones, can distort the image in the immediate vicinity.

tion this backscattering current has to be compensated for by the motion of electrons in the lower Landau levels similar to the case of the filling factor close to half-integer.[17] The electron flow in lower Landau levels causes a potential drop along the sample which is associated with the longitudinal resistance R_{xx}.

Let us now consider the effect of illumination. As was mentioned above, the photoexcited electrons enter the empty states of Landau levels and then recombine with holes. However, a photoexcited hole can also recombine with an electron in a lower fully occupied Landau level. As a result, this recombination effectively corresponds to the excitation of an electron from the lower to upper Landau level which can be described as the creation of a quasi-electron-hole pair in the two Landau levels (Fig. 8). Cyclotron-frequency radiation produces exactly the same effect. Hence, we can use the analogy with a *p-n* diode illumination by interband light and conclude that a photocurrent should appear as a result of the illumination of a "depletion" region between any two adjacent Landau levels, e.g., the upper ones as shown in Fig. 8. Its direction corresponds to electron flow from the edge to bulk of the 2D electron gas irrespective of the edge under illumination.

If the laser spot is at the edge with higher electron potential, the direction of the photocurrent coincides with that of the backscattering current considered above. This additional current will be compensated for by the electron flow in lower Landau levels, which results in increasing the longitudinal resistance. Obviously, the effect changes its sign at the other edge. The polarity of the bias current and of the magnetic field determines at which edge the electron potential is higher or lower. Hence, the edge effect in the images is in complete agreement with the edge-state model.[18,17] [A weak effect at the edge observed on the narrow sample at rather low bias currents (Fig. 5) implies the coexistence of responses from the edge and bulk.]

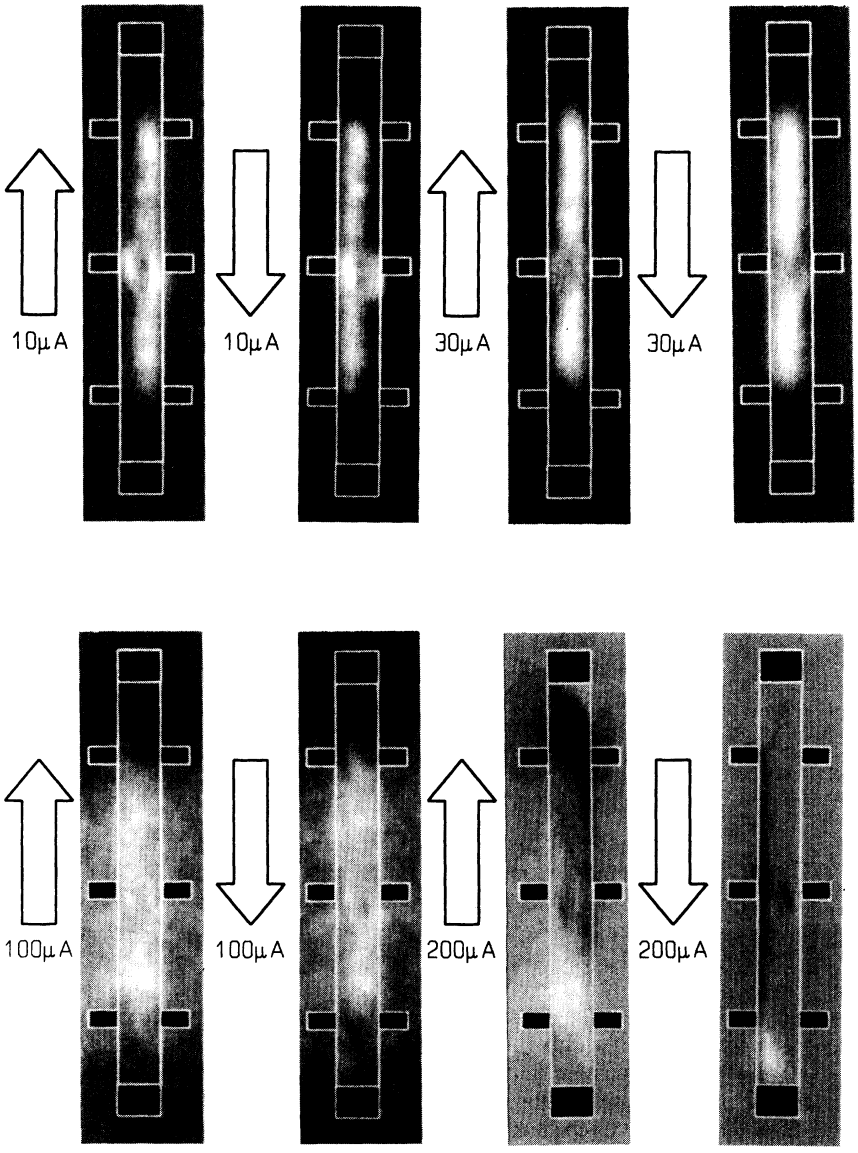

FIG. 6. Set of experimental images corresponding to the indicated current direction and size taken on the wide (250 μm) sample. The magnetic field of 4.3 T is directed into the plane of the diagram. The other conditions are the same as for Fig. 5.

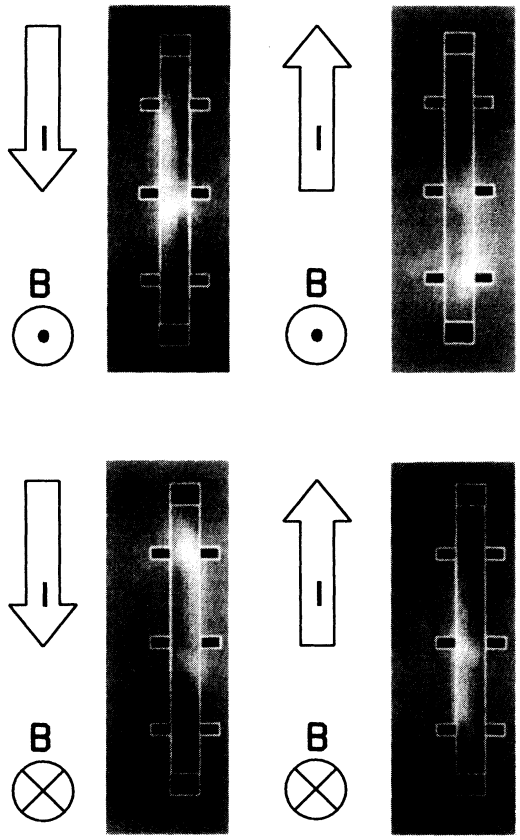

FIG. 7. Set of images corresponding to the four permutations of magnetic-field and current direction taken using the wide sample ($I=200$ μA, $B=4.3$ T, and resolution 50 μm). An increase in the longitudinal resistance (white) occurs when the light falls on the high potential edge of the sample.

As the bias current is increased, a larger part of electron backscattering current flows above the Fermi level through the upper Landau level. In other words, electrons are backscattered by diffusing through the upper Landau level and tunneling between quantum levels at the edges in a similar way to the case of filling factor close to half-integer.[13]

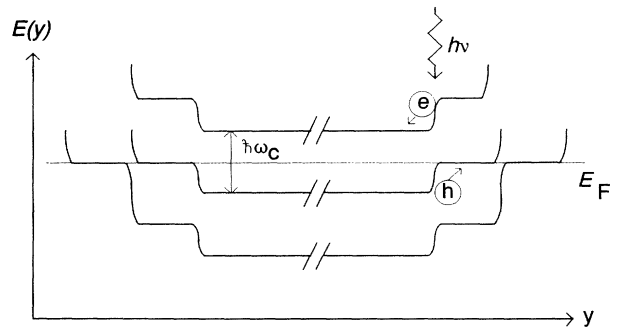

FIG. 8. Sketch of Landau levels at the sample edges in the case of a smooth confining potential. The Fermi level is in the energy gap. As a result of illumination quasi-electron-hole pairs are created on the Landau levels. When illuminating the region near the edge where there is a gradient of electron energy the photoexcited electrons enter the bulk of the 2D layer, as shown.

By further increasing the bias current the tunnel resistance drops, becoming small compared with resistance to the electron flow through the upper Landau level in the bulk. At these high currents, Landau levels are no longer decoupled and the edge effect disappears. Simultaneously, the heating of electrons increases and becomes a dominant process in the high-current region of the breakdown curve. As long as at these currents Shubnikov–de-Haas and photoresistance oscillations are not observable, the effect of illumination should be an *increase* of conductivity and consequently a *decrease* of the measured resistance (see Fig. 5). The onset of this latter behavior appears to scale approximately with the sample width which might be expected in the regime of uniform current distribution.

Finally let us consider the low-current region of the breakdown curve. It seems evident that the origin for QHE breakdown is the backscattering between opposite edge channels and, vice versa, the absence of backscattering in a finite region of filling factors leads to the QHE. (We do not consider the trivial case of an ideal 2D system without scattering.) So, the question is: *how does backscattering occur?*

We believe the heating effects can be excluded because, first, at low currents energy losses are very small and, second, heating effects are not seen in the intermediate-current region, as otherwise they would destroy the edge effect. In this range of currents the Hall potential drops and a change of chemical potential are too small to cause electron transitions from edge channels to the upper Landau level.

To explain the behavior of the breakdown curve and the experimental images, we have to conclude that the backscattering current flows at the Fermi level in a percolation picture due to random potential and follow the approach[19,20] developed in Ref. 10.

According to Ref. 10, the energy of the percolation threshold depends on the Hall electric field: the number of delocalized states in the Landau level grows with electric field. One can expect that the percolation threshold approaches the Fermi level when increasing bias current, which results in the appearance of the backscattering current and the QHE breakdown. In this case, a dependence of the backscattering current on the Hall potential difference should be strongly nonlinear. In a macroscopic sample, direct tunneling between edges of the sample is impossible; however, microscopic tunneling processes play an important role in formulating a quantum-percolation picture. In the presence of tunneling it is possible to observe hysteresis phenomena and sharp structures on the breakdown curve.[21,22] Indeed, we note that we observed some peculiarities on the breakdown curves for our samples. In particular, exact values of the longitudinal resistance changed slightly at the reversal of magnetic-field or bias-current direction. However, this did not affect the characteristic behavior of the breakdown curve that we discuss.

From the above considerations it follows that illumination will promote electron tunneling. Since the laser spot is large compared to the range of random-potential fluctuations, the effect of illumination will be an increase of local conduction, which results in an increase of the

backscattering current and the measured resistance.

As the bias current is increased further, the growth of backscattering current weakens. The bulk of a sample becomes less sensitive to illumination, which is accompanied by the growing edge effect (Figs. 5 and 6). Probably this behavior points out the importance of the screening effects of random potential.[16]

We note that the transient regions between quantum-Hall plateaus can also be treated as a result of the breakdown of the QHE. In this case, the backscattering current flows through the partially filled Landau level, as has been considered above. Whenever the electron transitions between Landau levels at the sample edges are suppressed, the backscattering current will decrease. This means that there is no fundamental difference between the "bulk" QHE and the so-called "anomalous" QHE discussed, e.g., in Ref. 16.

V. CONCLUSION

We have carried out spatially resolved measurements in the regime of QHE breakdown. The 2D images enable us to distinguish three characteristic stages of the breakdown that are consistent with the behavior of the breakdown curve $R_{xx}(I)$. First, the initial rise on the breakdown curve corresponds to a dominant response from the bulk of 2D layer: an increase of the resistance is observed in the images. Second, the growth of R_{xx} with increasing bias current slows and the edge effect appears in the images. The sign of the change in the resistance is opposite when illuminating opposite edges and is determined by the directions of current and magnetic field. Third, at high currents electron heating effects prevail. The rise of R_{xx} with increasing current speeds up again and the images indicate a decrease in the resistance under illumination. The experimental results enable us to identify the change of the percolation threshold in the Hall electric field leading to electron backscattering between the edges as the breakdown mechanism of QHE and to check the validity of the edge-state model.

ACKNOWLEDGMENTS

The authors would like to thank Mr. S. Chapman and Dr. K. R. Strickland for help with these experiments. The work was funded by grants from the SERC of the U.K. and the European Community.

*Permanent address: Institute of Solid State Physics, Chernogolovka, 142432 Russia.

[1]K. von Klitzing, G. Dorda, and M. Pepper, Phys. Rev. Lett. **45**, 494 (1980); M. A. Paalanen, D. C. Tsui, and A. C. Gossard, Phys. Rev. B **25**, 5566 (1982).

[2]G. Ebert, K. von Klitzing, K. Ploog, and G. Weimann, J. Phys. C **16**, 5441 (1983).

[3]S. Komiyama, T. Takamasu, S. Hiyamizu, and S. Sasa, Solid State Commun. **54**, 479 (1985).

[4]P. Streda and K. von Klitzing, J. Phys. C **17**, L483 (1984).

[5]K. Yoshihiro, J. Kinoshita, K. Inagaki, C. Yamanouchi, Y. Murayama, T. Endo, M. Koyanagi, J. Wakabayashi, and S. Kawaji, Surf. Sci. **170**, 193 (1986).

[6]P. C. van Son, G. H. Kruithof, and T. M. Klapwijk, Phys. Rev. B **42**, 11 267 (1990).

[7]O. Heinonen, P. L. Taylor, and S. M. Girvin, Phys. Rev. B **30**, 3016 (1984).

[8]L. Eaves and F. W. Sheard, Semicond. Sci. Technol. **1**, 346 (1986).

[9]E. Kuchar, G. Bauer, G. Weimann, and H. Burkhard, Surf. Sci. **142**, 196 (1984).

[10]S. A. Trugman, Phys. Rev. B **27**, 7539 (1983).

[11]A. J. Kent, D. J. McKitterick, L. J. Challis, P. Hawker, C. J. Mellor, and M. Henini, Phys. Rev. Lett. **69**, 1684 (1992).

[12]M. E. Cage, R. F. Dziuba, B. F. Field, E. R. Williams, S. M. Girvin, A. C. Gossard, D. C. Tsui, and R. J. Wagner, Phys. Rev. Lett. **51**, 1374 (1983).

[13]A. A. Shashkin, A. J. Kent, P. A. Harrison, K. R. Strickland, L. Eaves, and M. Henini (unpublished). In this manuscript we describe photoresistance imaging experiments carried out at half-integer filling factors. Edge effects are dominant in the images and from the location of the maximum edge response we are able to estimate the spatial extent of the edge channels.

[14]J. P. Bergman, Q. X. Zhao, P. O. Holtz, B. Monemar, M. Sundaram, J. L. Merz, and A. C. Gossard, Phys. Rev. B **43**, 4771 (1991).

[15]D. J. McKitterick, Ph.D. thesis, University of Nottingham 1993.

[16]B. Kane, Ph.D. thesis, Princeton University, 1988; A. M. Chang, Solid State Commun. **74**, 871 (1990); D. B. Chklovskii, B. I. Shklovskii, and L. I. Glazman, Phys. Rev. B **46**, 4026 (1992).

[17]V. T. Dolgopolov, G. V. Kravchenko, and A. A. Shashkin, Solid State Commun. **78**, 999 (1991).

[18]M. Büttiker, Phys. Rev. B **38**, 9375 (1988).

[19]S. Luryi and R. F. Kazarinov, Phys. Rev. B **27**, 1386 (1983).

[20]S. V. Iordansky, Solid State Commun. **43**, 1 (1982).

[21]M. E. Cage, Semicond. Sci. Technol. **7**, 1119 (1992).

[22]V. G. Mokerov, B. K. Medvedev, V. M. Pudalov, D. A. Rinberg, S. G. Semenchinski, and Yu. V. Slepnev, Pis'ma Zh. Eksp. Teor. Fiz. **47**, 59 (1988) [JETP Lett. **47**, 72 (1988)].

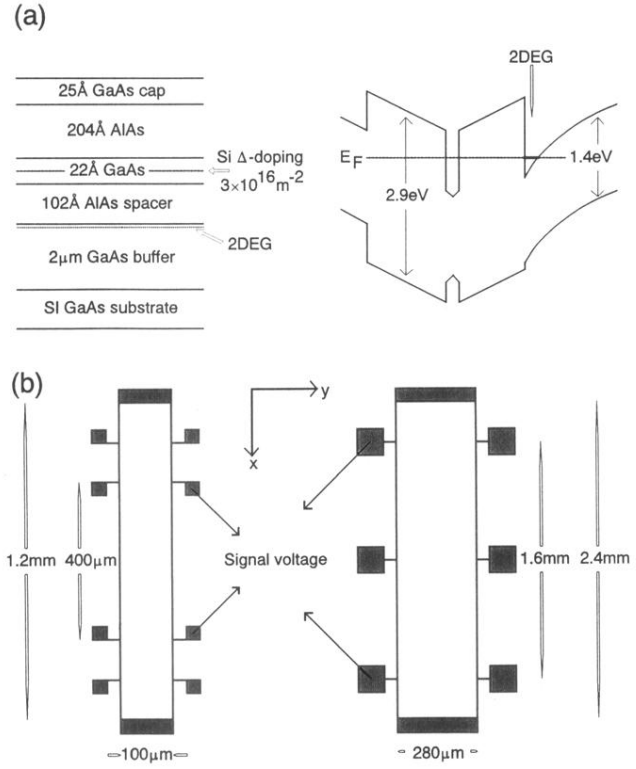

FIG. 2. (a) Cross section of the heterojunction and the band diagram. 2D electrons are supplied by the Si δ layer. The AlAs band gap shown in the Γ-valley conduction-band confining potential. (b) Geometry of samples used in measurements. Experimental results displayed in the following figures were obtained using the potential probes indicated. Axes indicate the scanning directions.

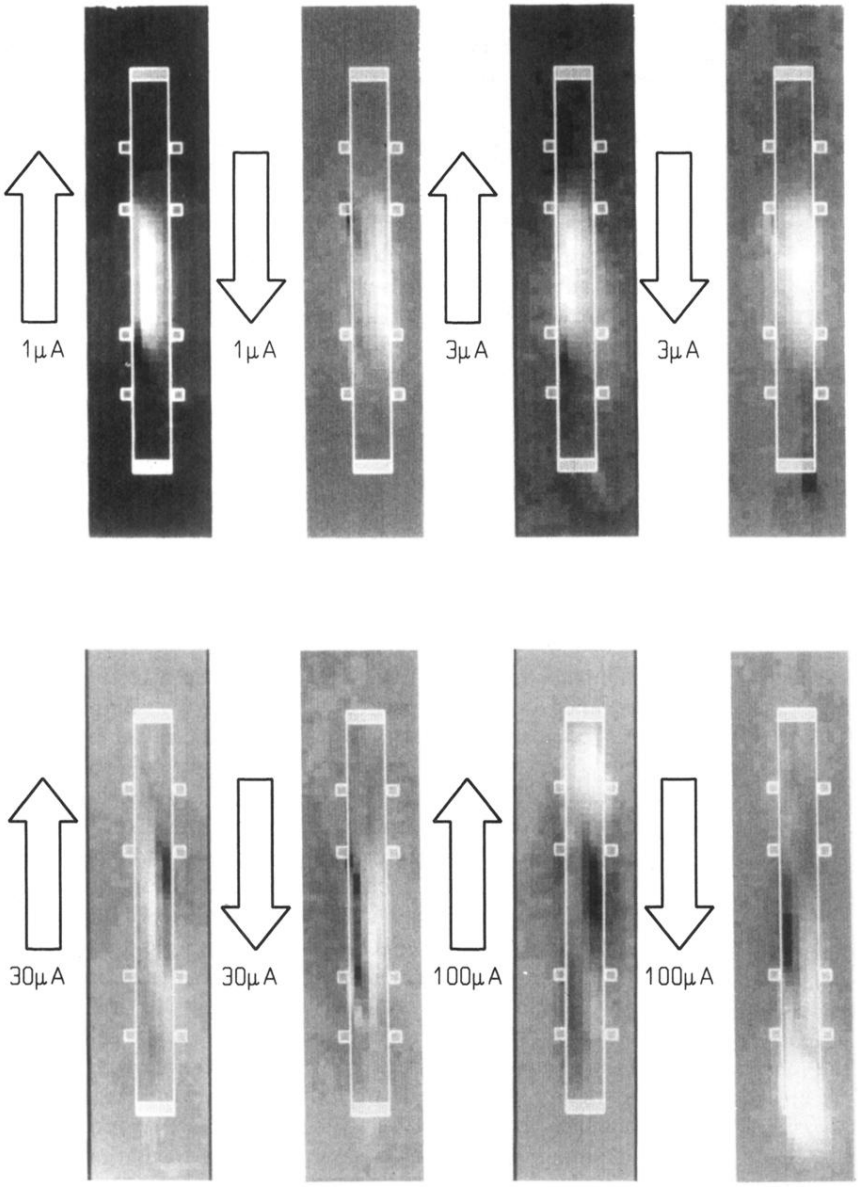

FIG. 5. A set of experimental images taken on the narrow (100-μm wide) sample at the indicated bias-current direction and size. The magnetic field of 4.6 T is directed into the plane of the diagram. White and black regions correspond, respectively, to an increase and decrease in R_{xx}; the zero level can be judged by looking at the shade at a position well outside the etched region. The images were taken at a resolution of 20 μm (five points across the width of the etched area). Sample contours with potential probes are also shown. It is noticeable that the presence of potential probes, even unused ones, can distort the image in the immediate vicinity.

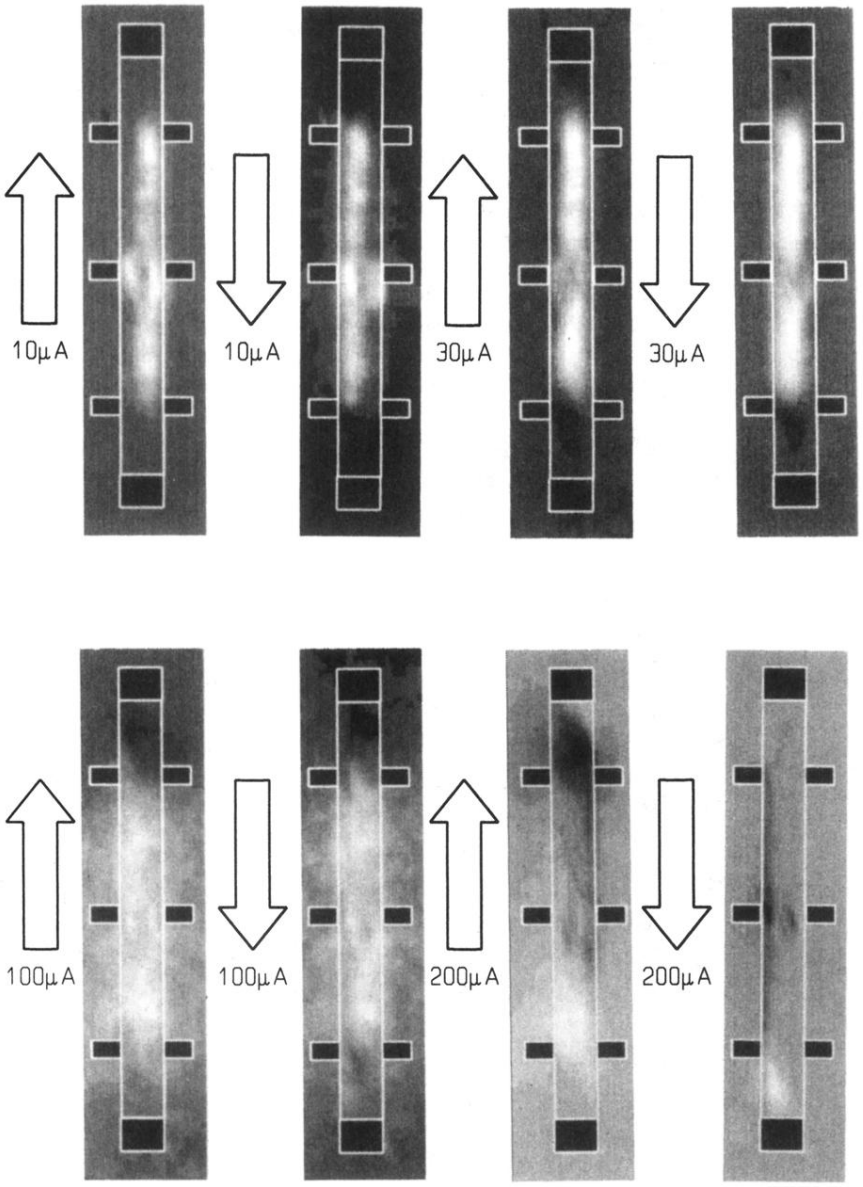

FIG. 6. Set of experimental images corresponding to the indicated current direction and size taken on the wide (250 μm) sample. The magnetic field of 4.3 T is directed into the plane of the diagram. The other conditions are the same as for Fig. 5.

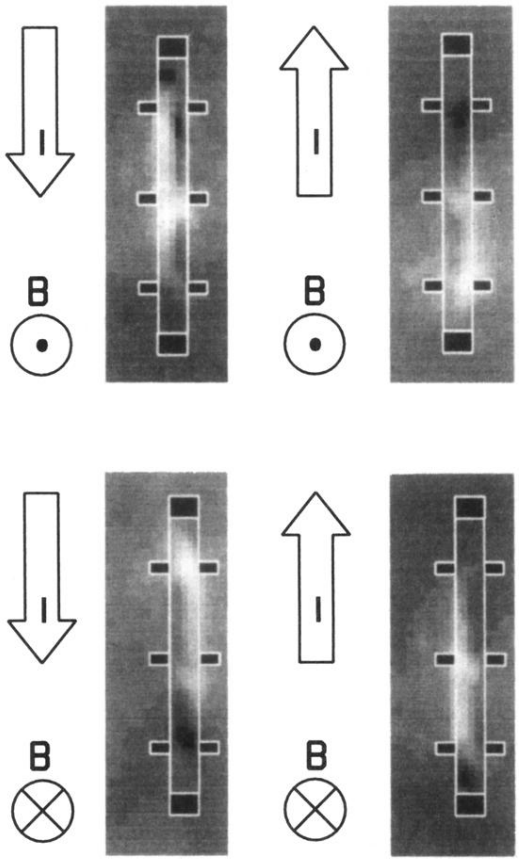

FIG. 7. Set of images corresponding to the four permutations of magnetic-field and current direction taken using the wide sample ($I = 200\ \mu$A, $B = 4.3$ T, and resolution 50 μm). An increase in the longitudinal resistance (white) occurs when the light falls on the high potential edge of the sample.